

Which Augmentation Should I Use? An Empirical Investigation of Augmentations for Self-Supervised Phonocardiogram Representation Learning

Aristotelis Ballas^a, Vasileios Papapanagiotou^b, Christos Diou^a

^a*Department of Informatics and Telematics, Harokopio University of Athens, Omirou 9, Tavros, 177 78, Athens, Greece*

^b*Department of Biosciences and Nutrition, Karolinska Institute, Blickagangen 16, Flemingsberg, 141 52, Stockholm, Sweden*

Abstract

Despite the recent increase in research activity, deep-learning models have not yet been widely accepted in several real-world settings, such as medicine. The shortage of high-quality annotated data often hinders the development of robust and generalizable models, which do not suffer from degraded effectiveness when presented with newly-collected, out-of-distribution (OOD) datasets. Contrastive Self-Supervised Learning (SSL) offers a potential solution to labeled data scarcity, as it takes advantage of unlabeled data to increase model effectiveness and robustness. However, the selection of appropriate transformations during the learning process is not a trivial task and often leads to degraded performance or even breaks down the ability of the network to extract meaningful information. In this research, we propose uncovering the optimal augmentations for applying contrastive learning, detecting abnormalities in 1D phonocardiogram (PCG) samples and thus learning a generalized representation of the signal. Specifically, we perform an extensive comparative evaluation of a wide range of audio-based augmentations, evaluate trained classifiers on multiple datasets across different downstream tasks, and finally report on the impact (positive and negative) of each augmentation in model training. We experimentally demonstrate that, depending on its training distribution, the effectiveness of a fully-supervised model can degrade up to 32% when evaluated on unseen data, while SSL models only lose up to 10% or even improve in some cases. We argue and experimentally demonstrate that, contrastive SSL pretraining can assist in providing robust classifiers which can generalize to unseen, OOD data, with-

out relying on time- and labor-intensive annotation processes by medical experts. Furthermore, the proposed extensive evaluation protocol sheds light on the most promising and appropriate augmentations for robust PCG signal processing, by calculating their effect size on model training. Finally, we provide researchers and practitioners with a roadmap towards producing robust models for PCG classification, in addition to an open-source codebase for developing novel approaches.

Keywords: Self-Supervised learning, Contrastive learning, Deep learning, Phonocardiogram classification, OOD representation learning

1. Introduction

Abnormal phonocardiogram (PCG) signals are often an important indicator of heart diseases or deficiencies linked to increased mortality [1]. The detection of such indicators in a non-invasive, accurate, and robust manner could assist towards prevention or timely treatment of such diseases, especially when access to healthcare services is limited.

Automated methods for detecting abnormal samples commonly rely on audio recordings; typically, audio is processed and then used to train classifiers that detect abnormal (i.e., non-healthy) samples and sometimes discriminate between different diseases (e.g., [2]). However, the audio quality of collected signals can be affected by several circumstances. While typical audio-related factors include microphone type or sampling rate, among others, for the case of PCG recordings additional factors can significantly affect the quality of their recording, such as placement of the microphone [3, 4], body size, skin, noise [5, 6], etc. The above cases can prove even more challenging, such as when screening an unborn child/fetus, where PCG can only be captured through the mother’s belly [7]. In addition to the quality of the recording conditions, the training of accurate ML models is heavily dependent on annotated data, the collection of which proves highly time- and cost-consuming. The above is especially important in the biomedical domain, where available samples are scarce to begin with.

As a result, classification models that have been trained on data originating from a single source or on low quality signals fail to generalize to previously unseen data distributions, which do not adhere to the i.i.d. assumption (i.e they are not independently and identically distributed), leading to degraded effectiveness [8, 9]. In this work, we propose training robust classifiers

for PCG signal classification by employing contrastive self-supervised learning (SSL) and investigate multiple combinations of augmentations, leveraging both labeled and unlabeled datasets. However, as the effectiveness of an backbone encoder trained via SSL heavily depends on the adopted augmentation policy [10], we also research the appropriate transformations to be applied on PCG signals and report their effect in model training. Specifically, we attempt to provide insight into the following research questions:

- Does contrastive SSL prove a valid training method for extracting robust and meaningful PCG representations?
- If so, which augmentations or transformations lead to such representations, proving the most effective, and which actually inhibit training?
- Is a classifier trained on the above representations able to maintain adequate effectiveness and demonstrate generalization capabilities when evaluated on OOD data, in contrast to its fully supervised counterpart?

To answer the above research questions, we develop and implement an extensive comparative evaluation in which we: (a) investigate multiple combinations of augmentations, leveraging both labeled and unlabeled datasets, (b) examine the effectiveness on a global “normal vs. abnormal” downstream task, as well as downstream tasks specific to each dataset (where applicable), (c) evaluate all trained classifiers on OOD data that are left-out during training, and finally, (d) calculate the effect size of each augmentation. To the best of our knowledge, this is the first paper researching the effect of each applied augmentation on learning robust OOD PCG representations. To facilitate further research in the field and provide a comprehensive baseline, we have open-sourced our codebase¹.

The rest of the paper is organized as follows. Initially, section 2 presents previous work on PCG-based classification, SSL training, and model robustness. Followingly, section 3 presents the methodology, including training approach, network architecture, augmentations, and datasets. Finally, section 4 presents the evaluation framework and results, while section 5 concludes the paper.

¹Code available at: <https://github.com/aristotelisballas/listen2yourheart>

2. Related Work

Accurate and robust PCG classification has major implications in the well-being of patients since it can often be an indicator of heart deficiencies. However, the limited availability of annotated data has hindered the progress of research in the field, along with biosignal classification in general. In this section, we focus on the most important papers and previous works in DL for PCG classification and in SSL for 1D biosignal processing. We also refer to methods which have been specifically developed for robust 1D biosignal classification.

2.1. Deep Learning for Phonocardiogram Classification

The release of publicly available PCG datasets under the scope of the 2016 [11] and 2022 [12] PhysioNet [13] challenges, has sparked a line of research in deep learning for PCG classification. The majority of previous works have mainly proposed either 2D or 1D CNN architectures for tackling this particular problem. The main difference lies in whether the proposed models are trained directly on the one dimensional recorded auscultation waves or on spectral images extracted from the audio recordings. For example, multiple recent papers [14, 15, 16, 17] propose combining mel-spectrogram images extracted from PCG signals with encoded patient demographic data, in a dual-branch CNN model. The authors find that the combination of the above representations leads to improved accuracy in the heart murmur detection task. Similarly, in another work utilizing frequency domain features, the authors of [18] design a hierarchical deep CNN architecture that extracts and combines features from multiple-scales of PCG Mel-Spectrograms. A more recent work, [19], proposes training an ensemble of 15 ResNets [20] with channel-wise attention mechanisms on similar spectrograms, for grading murmur intensity in PCG recordings.

Although few, 1D models also prove promising in the heart-murmur detection domain. In [21] the authors employ a transformer-based neural network and train it on 1D wavelet power features extracted from raw PCG signals. On the other hand, [22] proposes using a U-Net to predict heart states from the raw PCG signal and combine the predictions with a ResNet model for the final classification. In a different approach, the authors of [23] suggest that the combination of a 1D CNN-Bi-LSTM model coupled with attention mechanisms, trained in conjunction with a feature-based classifier leads to robust abnormal PCG signal detection.

In this work, we build upon our preliminary research [24] for the 2022 PhysioNet challenge. In particular, we demonstrate the value of adopting self-supervised contrastive learning for robust PCG classification and also report the top augmentations which should be implemented in such a framework. To our knowledge, this is the first study extensively researching the benefits of each augmentation, and their combinations, for contrastive SSL in 1D PCG signal processing. The aim of this study is to provide future researchers with best-practices regarding PCG signal augmentation, while also propose a structured protocol for the evaluation of developed methods.

2.2. Self-Supervised Learning in 1D biosignal classification

Self-supervised representation learning (SSL) [25] was initially proposed for diminishing the limit posed by the requirement of large annotated datasets for practical and production-ready deep learning systems. By taking advantage of common features present in unlabeled data, SSL approaches rely on pretext tasks [26] to exploit them and ultimately provide models which are able to extract generalized and robust representations. Inspired by advancements in contrastive predictive coding [27], the goal of Self-Supervised Contrastive Learning [28, 29] is to train a model to recognize augmented or transformed views of the same initial signal. By distinguishing between representations which originate from different original signals, the resulting model is able to extract invariant representations from its input data and reason upon features which remain stable across distinct data distributions [30]. The SSL paradigm seems to fit quite well in the medical and healthcare domain. In a field where sufficient annotated datasets are scarcely available, there proves a need to provide systems which can take advantage of the small amount of data but also yield adequate and trustworthy inference results. To this end, several works have proposed SSL approaches for processing biosignals in the past, the majority of which have studied its advantages when extracting representations from either electroencephalography (EEG), electrocardiography (ECG) or electromyography (EMG) signals.

Regarding EEG signals, several prior studies revolve around developing methods for emotion recognition and/or sleep stage detection [31]. The authors of [32] propose augmenting multi-channel EEG signals by recombining several channels into additional channels which represent different aspects of the EEG recording. On top of the combination, they augment each channel by applying pre-defined transformations and employ a contrastive loss for improved emotion recognition and sleep-stage classification. In another

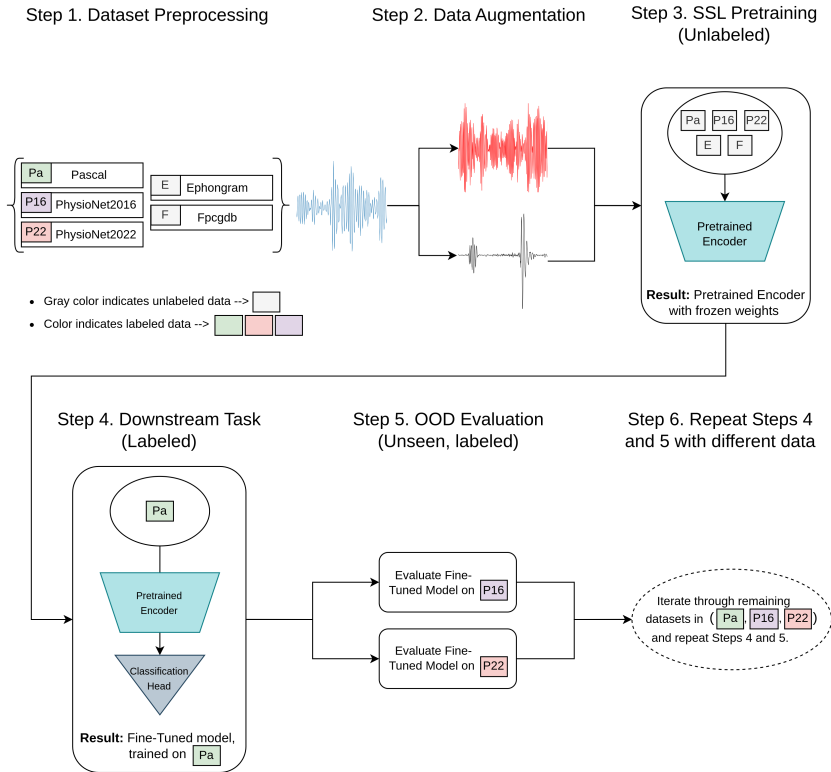


Figure 1: Illustration of the proposed experiment pipeline for training and evaluating the effectiveness and robustness of a model trained via Self-Supervised Contrastive Learning for PCG classification. The framework has six steps. In the first step, all datasets are prepared and homogenized into a common format, as described in Section 3.1. In the second step, each signal is augmented to two versions. In the next step, the unlabeled and augmented signals are used to train the backbone encoder (Fig. 2 left) to maximize the agreement between representations originating from the same initial signal. Following the pretraining phase, in step 4, a classification head (Fig. 2 right) is attached to the frozen weights of the pretrained encoder. The classifier weights are fine-tuned on data drawn from one of the Pascal, PhysioNet2016 or PhysioNet2022 datasets, in a fully supervised manner. The final model is then evaluated on the test split of the same dataset. In the fifth step of the framework, the generalization ability of the fine-tuned model is assessed on signals drawn from datasets which are left-out (“unseen”) during the training process in step 4. We argue that given sufficient data and appropriate augmentations, the pretrained encoder will be able to extract a generalized PCG representation regardless the dataset. Finally, we repeat the fine-tuning and OOD evaluation steps for each remaining dataset (step 6), to assess the robustness of our method when the classifier has been trained on different signal distributions.

work, the authors of [33] argue that a model can learn informative EEG representations by predicting whether two windows of a signal are sampled from the same temporal context and use the above reasoning to design a relevant pretext task. The above study is extended in [34] where contrastive predictive coding is implemented on similar SSL-learned features to both predict sleep-stages and detect pathologies in multi-channel EEG signals. Finally, [35] proposed BENDR, which combines attention mechanisms [36] and contrastive learning to produce a model with increased generalization capabilities and fine-tune it for several downstream tasks in the EEG biosignal domain.

Several SSL methods have been proposed for ECG signal analysis as well [37], most of which focus on either emotion recognition or pathology detection. For example, in [38] the authors argue that the training of a model to recognize different ECG signal transformations can lead to generalized and robust feature learning. They evaluate their method on four emotion recognition datasets and report state-of-the-art results. In another paper studying emotion recognition from ECG signals, [39] introduces a transformer model which is pretrained to predict masked values of the signal and then fine-tuned to predict the level of emotion in individuals. Regarding the pathology detection task, most prior works focus on discriminating normal ECG signals from others indicating a type of arrhythmia. Among the self-supervised approaches proposed for ECG pathology detection, contrastive learning is the most prevalent choice. Specifically, authors either propose exploiting the temporal and spatial invariances of the ECG signal [40], implementing attention mechanisms [41] or combining wavelet transformations and random crops of the signal [42] for the pretext contrastive task, before fine-tuning their resulting models for arrhythmia detection. In a different approach, [43] propose learning good representations by contrasting signals both at the inter- and intra-subject levels. Specifically, they argue that similarity should be maximized between signals which share a common label but are measured from different individuals.

Finally, EMG signal processing is another interesting field which would greatly benefit from the application of robust prediction models [44]. For example, [45] introduces NeuroPose, a system for 3D hand pose tracking which aims to alleviate the problems imposed due to different sensor mounting or wrist positions, by pretraining an encoder-decoder model to recognize augmented views of a single user’s signal and then finetuning a downstream model to a subset of signals from a separate user. Similarly, the authors

[46] employ a contrastive loss to pretrain a model on EMG signals for hang-gesture recognition.

2.3. Model Robustness in 1D biosignal classification

Extracting generalized and robust representations has been one of the most important long-standing goals of machine learning [47]. To test and improve the generalizability prowess and robustness of deep learning models, several fields have emerged, such as Domain Adaptation [48], Transfer Learning [49], and Domain Generalization [50, 9, 51], which use data from non-i.i.d. distributions or out-of-distribution (OOD) data for model evaluation. These distinct data distributions are referred to as data *Domains*, as they are most often the outcome of different data generating processes. Here, we reference prior works which fall under the above research fields.

Domain adaptation (DA) methods are the most popular choice when aiming to produce models with improved generalization capabilities in 1D biosignal classification. Similar to *Transfer Learning* (TL), DA algorithms leverage the representation learning capabilities of models pretrained on diverse source data distributions and fine-tune them on previously unseen but similar target distributions. The end-result is a model which remains robust under the distribution shift between source and target data. In healthcare, DA methods are proposed for a plethora of biosignal classification tasks. In [52], the authors propose pre-training vanilla CNN networks on a large corpus of raw ECG signals and demonstrate their effectiveness when fine-tuned on a smaller dataset for arrhythmia detection. In another more recent work, He et al. [53] propose tackling the distribution shift between different arrhythmia detection ECG datasets, by employing three distribution alignment mechanisms. To be more specific, they first extract spatio-temporal features from preprocessed signals, pass them through a graph convolutional neural network and finally align the resulting representations between source and target domains. Many studies have researched the advantages of DA and TL in EEG classification as well [54]. To name a few, the authors of [55, 56] and [57] propose aligning source and target distributions via adversarial learning for motor image EEG classification and epilepsy detection respectively, while [58] investigates several state-of-the-art DA algorithms for EEG-based emotion recognition.

Finally, *Domain Generalization* algorithms aim to tackle the model generalization at its core, as the main goal is to provide generalized models that perform well across unseen datasets. Although limited, there has been a

recent interest in biosignal DG research. In the field of PCG classification, the authors of [59] propose a ensemble classifier fusion method yields improved results in a DG setup for abnormal vs normal signal classification. To tackle the domain shift and variability present in ECG signals collected from different patients, [60] and [61] propose domain-adversarial model training for ECG and EEG classification, respectively. Most recently, the authors of [9] introduce a DG benchmark and a model which leverages representations from multiple layers of the network, inspired from [62], for 12-lead ECG and 64-channel EEG classification.

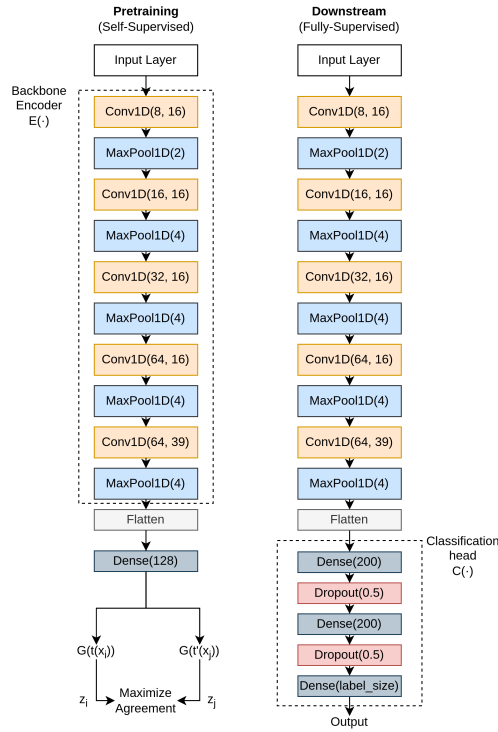


Figure 2: The architecture of the CNN encoder trained via SSL contrastive learning (left) and the classification head trained for the downstream task (right). The weights of the encoder or "backbone network" are frozen after the pretraining phase. During the downstream task, the classification head is attached to the pretrained encoder and its weights are fine-tuned on the dataset of said task in a fully-supervised manner. The architecture of the "downstream model" is used as a baseline in all of our experiments, where all of its layer weights are adjusted during fully-supervised training.

3. Materials and Methods

We introduce an evaluation framework for assessing both the combination of various transformations and the robustness of a network trained via contrastive SSL, against a fully supervised baseline model. This allows us to evaluate and report on the most promising signal transformations or augmentations, for the PCG classification domain, while also highlight additional benefits of training an end-to-end classification model via Self-Supervised Contrastive Learning, such as improved model robustness and generalization.

For the self-supervised training of all models, we adapt the SimCLR [63] methodology for 1D PCG representation learning and then evaluate numerous augmentation combinations designed specifically for 1D signal processing tasks.

In the following sections, we describe the datasets and preprocessing steps followed for all signals included in the study, and describe in detail the protocol followed for evaluating the significance of each combination of augmentations, as well as the generalization ability of a model pretrained with self-supervised contrastive learning. Finally, we present the architecture and relevant implementation details of the 1D CNN network implemented for PCG classification.

3.1. Datasets & Downstream tasks

The PCG signals used in this study originate from a total of 5 distinct public datasets and are available as “wav” files. These include the Ephnogram [64], FPCGDB [65], Pascal [66], PhysioNet2016 [11], and PhysioNet2022 [12] databases. Here we describe each dataset separately and provide all necessary details regarding the preprocessing steps followed for the homogenization of all signals into a common format.

The **Ephnogram** [64] database contains a total of 69 multi-channel, simultaneous ECG and PCG recordings from 24 healthy adults aged between 23 and 29, acquired during physical activity and rest conditions. Most recordings (62 during exercise) are 30min long, while the duration of the remaining 7 (rest) is about 30 seconds. As specified by the researchers, the dataset includes poor sample signals for noise research purposes. As this dataset was proposed and gathered for multi-modal signal processing purposes and not for pathology detection or classification, it does not include labeled samples.

For our study, we use the unlabeled samples of the PCG signals for the SSL pretraining of our models. All PCG recordings were sampled at 8 kHz.

The **FPCGDB** [65] or Fetal PCG Database, as its name suggests, is a dataset containing 26 20-minute fetal phonocardiographic signals, gathered from healthy women during their the remaining months of their pregnancy and sampled at 333 Hz. Similarly to the Ephnogram dataset, the collected signals were obtained for the development of fetal PCG signal simulation and fetal heart rate extraction algorithms. Hence, this dataset also does not contain any labeled samples for classification purposes. Furthermore, most recordings are somewhat corrupted by noise, either due to the pregnant human body which contains various noise sources, such as muscular movements or placental blood turbulence, or even due to the surrounding environment.

The **Pascal** [66] Heart Sound Classification challenge was introduced for developing algorithms for the automatic screening of cardiac pathologies. The challenges contains two tasks; one for heart sound segmentation and one for classification. In our work, we use the publicly available labeled data for model training and evaluation which was gathered in both clinical and in-the-wild settings. Notably, the 832 PCG signals are classified as either Normal, Murmur, Extra Heart Sound, Artifact or Extrasystole². The recording lengths vary from 1 to 30 seconds and are sampled at 195 Hz. As each sample is annotated with a single label, the above task is a multi-class classification problem.

The remaining two datasets were also introduced in the context of public challenges for PCG classification. Similarly to the Pascal challenge, the objective of the **PhysioNet2016** [11] challenge aims at urging researchers to develop robust algorithms for differentiating normal and abnormal heart sound recordings but instead introduces a binary classification problem. The data included for model training in the dataset contains a total of 3,126 PCG recordings collected from a single precordial location from both healthy subjects and patients suffering from a variety of heart defections, lasting from 5 to around 120 seconds. Once again, the recordings were gathered in both clinical and non-clinical environments, with a sample rate of 2 kHz.

Finally, the **PhysioNet2022** challenge [12] was designed for the development of algorithms which could detect heart murmur in PCG signals. Succe-

²Each different category is described in the official challenge description (<https://istethoscope.peterjbentley.com/heartchallenge/index.html>).

dent to the 2016 challenge, the 2022 challenge contains multiple heart sound recordings, collected from multiple auscultation locations. The available data includes 3,163 recordings from 942 patients in total. Each patient has one or more PCG signals, recorded from one of the four heart valves or from a separate prominent auscultation location. Each of the recordings can be classified as "present", "absent" or "unknown", meaning that heart murmur presence can be either detected, not detected or can not be determined (e.g due to noise or corrupted audio) respectively, rendering the challenge a multi-class classification problem. The sampling rate of the above signals is 4 kHz.

Each dataset contains signals of varying length, sampling rate and label classes. To accommodate model training in our framework, we follow a similar process as in [24] for converting all signals into a similar format. As a first step, to avoid transient noise artifacts, we initially discard the first and final 2 seconds of each PCG recording. The resulting signal is split into 5 second overlapping windows with a 50% overlap. After resampling all samples to 2 kHz, we assign two types of labels to each window; one that follows the annotations of its original dataset (if it is drawn from a labeled dataset) and one binary label indicating whether it derives from a normal heart sound recording or not³. For the SSL pretraining stage, we assign pseudolabels to each window, as described in Section 3.2. The assignment of binary labels to each window enables the evaluation of trained models across datasets, which do not necessarily share similar sample classes. For example, a classifier trained to detect normal PCG signals in the Pascal dataset, can be then evaluated without further training on samples from the PhysioNet2022 dataset. The above evaluation process is described in detail in Section 3.4.

3.2. Self-Supervised Contrastive Learning for PCG Representation Learning

The main goal of this study is to, first of all, verify the use of SSL contrastive learning and also evaluate the importance of augmentation selection, for robust PCG representation learning. The proposed framework consists of two separate tasks, a *Pretraining* pretext task and a *Downstream* task, as depicted in Figure 1.

Assume a 1D PCG signal $x \in \mathbb{R}^{1 \times L}$ sampled from \mathcal{X} , where L is the length of the signal. The aim of the contrastive SSL pretext task is to learn robust representations of x from unlabeled PCG signals, by maximiz-

³In this study, all recordings initially labeled as *unknown* are considered abnormal.

ing the agreement between two different augmented versions of itself (positive pair) and simultaneously minimizing the agreement between entirely separate augmented windows. Essentially, a model is trained to predict whether two augmented signals are the result of different transformations applied on the original sample. Formally, let $t(\cdot)$ be a transformation or augmentation function drawn from a family of functions \mathcal{T} . During the pretraining phase, an audio window x is augmented to two different versions \tilde{x} and \tilde{x}' , after the application of two transformation functions $t \sim T$ and $t' \sim T'$ respectively. Therefore, an initial batch of N sample windows $(\tilde{x}_1, \tilde{x}_2, \dots, \tilde{x}_n)$ results into an augmented batch of $2N$ signals $(\tilde{x}_1, \tilde{x}_2, \dots, \tilde{x}_n, \tilde{x}'_1, \tilde{x}'_2, \dots, \tilde{x}'_n)$, where $\tilde{x}_i = t(\tilde{x})$ and $\tilde{x}'_i = t'(\tilde{x}_i)$ for $i \in [1, N]$. As mentioned, each augmented pair of signals resulting from the same original window is considered a positive pair, e.g. $(\tilde{x}_1, \tilde{x}'_1)$, while pairs of different original windows comprise negative pairs, e.g. $(\tilde{x}_1, \tilde{x}'_2)$. Following its augmentation, the $2N$ signal batch is passed through a neural network encoder model $E(\cdot)$ (Figure 2), where each signal is encoded into a representation $\tilde{h} = E(\tilde{x})$. Subsequently, the resulting representations are flattened and passed through a fully connected linear layer $G(\cdot)$ and projected into 128-dimensional vectors $\tilde{z} = G(\tilde{h})$.

For the *contrastive prediction* task, we employ the contrastive *NT-Xent* loss function introduced in [27] and implemented in the SimCLR framework [67]. Specifically, given a set $\{\tilde{x}_k\}$ which includes an augmented positive pair \tilde{x}_i and \tilde{x}_j , a model trained via contrastive SSL aims to identify \tilde{x}_j in $\{\tilde{x}_k\}_{k \neq i}$ for a given \tilde{x}_i . The contrastive loss for a positive pair $(\tilde{x}_i, \tilde{x}_j)$ is formulated as follows:

$$\ell_{i,j} = -\log \frac{\exp(\text{sim}(\mathbf{z}_i, \mathbf{z}_j)/\tau)}{\sum_{k=1}^{2N} \mathbb{1}_{k \neq i} \exp(\text{sim}(\mathbf{z}_i, \mathbf{z}_k)/\tau)}, \quad (1)$$

where N is the initial batch size of the randomly sampled signals, $\mathbb{1} \in [0, 1]$ is an indicator function and τ a temperature parameter. The $\text{sim}(\cdot)$ function calculates the cosine similarity between the encoded vectors and is defined as:

$$\text{sim}(\mathbf{z}_i, \tilde{\mathbf{z}}_i) = \frac{\mathbf{z}_i \cdot \tilde{\mathbf{z}}_i}{\|\mathbf{z}_i\| \|\tilde{\mathbf{z}}_i\|}. \quad (2)$$

The final loss is computed across all positive pairs in a mini-batch.

After the pretraining step has been completed (i.e., step 2 in Figure 1), the weights of the backbone encoder network $E(\cdot)$ are frozen. At this point,

the model is expected to produce a robust representation \tilde{h} . While keeping the weights of the encoder frozen, a classification head $C(\cdot)$, with randomly initialized weights, is attached to the pretrained network. The layers of the classification head are then trained on labeled audio windows (x, y) in order to predict labels for each downstream task. The classification layers are trained via fully supervised learning, with the categorical Cross-Entropy (CE) loss. Depending on the labels of each dataset in the downstream task, the CE loss is reduced to its binary form.

3.3. Augmentations for PCG Representation Learning

Arguably, the most integral part of the proposed framework is the family of transformation functions \mathcal{T} , which is applied on each audio window, as the type and intensity of each function can drastically affect the learning of the encoder network. In order to conduct a rigorous evaluation of all augmentations included in the proposed contrastive SSL framework and also report the functions which should most likely be applied for robust PCG representation learning, we select to implement functions that either simulate factors that can be found in real world scenarios. For example, the first thing that comes to mind is the volume of noise polluting recordings during PCG collection. Additionally, the difference in sensor conductance can lead to different scales of the recorded signals. To this end, it would make sense to at least either add artificial noise to randomly scale each audio window during the pretraining task. Following the above rationale, in our study we select to implement and evaluate the effectiveness of a total of 6 different augmentations, each of which is described below:

- **Noise:** Zero-mean Gaussian Noise is added to the PCG signal. Specifically, given noise $n(t) = \frac{1}{\sqrt{2\pi}\sigma} e^{-\frac{(x-\mu)^2}{2\sigma^2}}$, where μ is the mean and σ the standard deviation, the resulting signal is $\tilde{x}(t) = x(t) + n(t)$.
- **Cut-off Filters:** Here either a high-pass or low-pass filter is applied to the signal, at a 250, 500 or 750 Hz cutoff.
- **Scale:** The signal is randomly scaled by a factor of $a \in [0.5, 2.0]$ to yield $\tilde{x}(t) = a \times x(t)$.
- **Reverse:** The signal sequence is reversed.

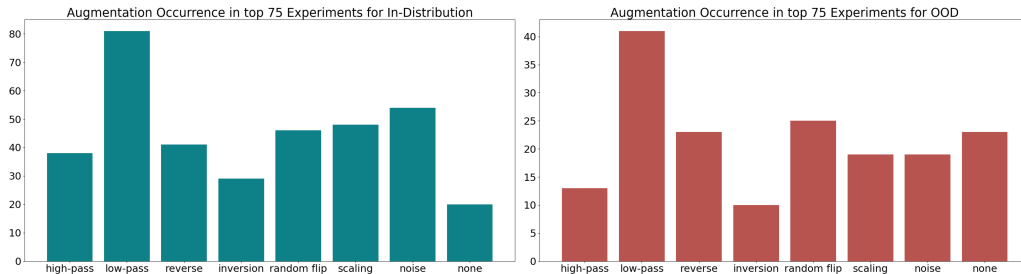


Figure 3: Number of occurrences of each augmentation type in the top 75 performing models in each downstream task, leading to 150 total augmentation pairs. This offers an indication on the importance of each augmentation across all experiments. The plot on the left presents the result for In-Distribution experiments, while the plot on the right the results for the OOD experiments.

- **Inversion:** As its name suggests, this transformation inverts the original signal by multiplying it by -1, i.e., $\tilde{x}(t) = -x(t)$.
- **Random Flip:** This function takes as input the signal and concurrently applies the ‘reverse’ and ‘inversion’ augmentations based on a given probability (p) between 0.3, 0.5 and 0.7.

In the proposed framework, we also evaluate the composition of augmentations by applying one transformation after the other. Specifically, we consider 4 different augmentation cases: 0vs1, 1vs1, 1vs2 and 2vs2. In each case, the signal is either not transformed, transformed once or augmented by the application of 2 concurrent functions.

3.4. Evaluation Protocol

The present study aims at providing future researchers with a roadmap for applying SSL in Phonocardiogram processing problems. To this end, we design a rigorous and comprehensive protocol for evaluating the importance of each applied augmentation in robust PCG classification. Each different augmentation combination is evaluated by repeating the experiment illustrated in Figure 1, with the exact same data splits for fair comparison.

In the first step of the framework, we create a pool of 5 sec unlabeled audio windows from all available datasets, namely Pascal, PhysioNet2016, PhysioNet2022, Ephnogram and Fpcgdb. After the preprocessing step has been completed and all signals are homogenized in the common format described in Section 3.1, they are randomly shuffled and split into training and

validation splits (80% and 20% respectively). In the second step, the split signals are cut into batches. Each sample in the batch is then duplicated and augmented by applying either one or a combination of the functions described in Section 3.3. The augmented samples are then passed through a Neural Network encoder, which is trained via the contrastive pretraining task (Step 3). After the SSL backbone model has been trained, its weights are frozen.

In Step 4, a classification head with learnable weights is attached to the pretrained encoder which is then trained on data from one of the labeled datasets (Pascal, PhysioNet2016 or PhysioNet2022). Specifically, each of these datasets is split into training, validation and test splits with a standard 70%-20%-10% ratio and the trained model is evaluated on the test split only. Since each model is evaluated on test data originating from the same distribution as its training data, we call this the "In-Distribution" evaluation. Inspired by recent work in biosignal domain generalization [9], we also design an evaluation protocol for assessing the robustness of a trained classifier on out-of-distribution data, which are drawn from entirely different datasets. Since the data has been completely left-out during downstream training, the above process is followed for evaluating the generalization ability of a model. Specifically, we now also freeze the weights of the attached classification layers and test the model on data drawn from the remaining 2 labeled datasets. For example, if the network is trained for the Pascal downstream task, it is evaluated on both in-distribution data (Pascal) and on out-of-distribution data (PhysioNet2016 and PhysioNet2022). We call this step the out-of-distribution or OOD evaluation step. However, in order to evaluate the same model on each separate dataset, all data must share common labels. To that end, we implement two different downstream task types: 'All' and 'Binary'. In the 'All' downstream task, the original labels of each dataset are assigned to each audio window, while in the 'Binary' task a signal is labeled as either 'normal' or 'abnormal', as described in Section 3.1. In the case of the PhysioNet2016 dataset, the two tasks match as it introduces a binary classification problem in the first place. For a fair comparison, all test data splits remain the same across each evaluation scheme. Finally, to assess the pretrained backbone encoder (and therefore the applied augmentations) on all available data, we repeat Steps 4 and 5 with the remaining datasets in a round-robin fashion (step 6 of the proposed framework).

To thoroughly evaluate the proposed method we also repeat the entire experiment by leaving data out during Step 1 and pretraining the model with

fewer data. This is also a means to concretely evaluate the proposed method on true OOD data, as they are completely hidden throughout the training process, either pretraining or downstream training. The best augmentation combinations are selected based on the effectiveness of the downstream models on the ‘In-Distribution’ test split. The same models are then evaluated on the hidden ‘OOD data’.

3.5. Implementation Details

In this section, we describe all the implementation details regarding the execution of our experiments. First of all, for the backbone encoder model we implement the same model used in [24] and [68]. The encoder model is a 5 layer convolutional neural network, the architecture of which is depicted in Figure 2 (left).

For the contrastive SSL pretraining phase, we train the conv layers of the network by projecting the output of the last layer into a 128-D space via a dense or fully-connected layer and minimize the NT-Xent loss (eq. 1). For the cosine similarity (eq. 2) we use a temperature of 0.1, as in [24], while the initial batch size is set to 256 (leading to 512 after augmentation occurs). The SSL training epochs are set to a maximum of 200 epochs, based on an early stopping set on the validation split with a patience of 10 epochs. Additionally, to accommodate the large batch size we employ the LARS optimizer [69] with a linear learning rate warm-up of 20 epochs, up to 0.1, followed by a cosine decay of 1%.

During the downstream task, the dense projection layer of the pretrained encoder is discarded and all convolutional weights are frozen. Next, a 3-layered classification head is appended to the pretrained network, as shown in Figure 2 (right). Dropout layers are also included between the dense layers of the classification head for further improving model robustness. The output size of the last decision layer depends on the downstream task type and the label size in each dataset. For the ‘Binary’ type and the PhysioNet2016 dataset, the output size is set to 1. For the ‘All’ type, the output size is set to 5 or 3, for the Pascal and PhysioNet2022 datasets respectively. In all cases, the classification head is trained via the appropriate cross-entropy loss and the Adam optimizer. Additionally, the learning rate is set to 10^{-4} and the batch size is set to 32. Once again, we train the model for 100 epochs at most, using early-stopping with 20 epochs patience. The same CNN model is used for the fully-supervised baseline. All experiments are implemented

Table 1: The effect size of each augmentation on the SSL contrastive training. The effect were measured based on the out-of-distribution micro F1 scores for the PhysioNet2016 dataset, when trained on signals from PhysioNet2022, sorted by effect size. LP and HP indicate Low and High Pass filters, respectively.

Augmentation	Cohen’s d (\uparrow)
Random Flip (0.5)	1.80116
Cut-off (500, 450) (LP)	1.32952
Cut-off (750, 700) (LP)	1.2839
Cut-off (250, 200) (LP)	1.26386
Random Flip (0.3)	0.57836
Random Flip (0.7)	0.49227
Scale (1.0, 1.5)	0.20685
Noise (-0.01, 0.01)	0.11594
Inversion	-0.00088
Reverse	-0.00398
Scale (1.5, 2.0)	-0.11695
Cut-off (500, 550) (HP)	-0.1149
Cut-off (250, 300) (HP)	-0.2079
Noise (-0.001, 0.001)	-0.23983
Noise (-0.1, 0.1)	-0.32574
Scale (0.5, 2.0)	-0.40168
Cut-off (750, 800) (HP)	-0.47433

in Tensorflow 2.12 [70] and trained on a SLURM [71] cluster, containing 4×40GB NVIDIA A100 GPU cards, split into 8 20GB virtual MIG devices.

4. Results and Discussion

4.1. Augmentation and Transformation Evaluation

To avoid the combinatorial explosion poised by the evaluation of all possible augmentation combinations, we designed a protocol to limit the experiments to a feasible amount. As mentioned in Section 3.3, there are a total of 7 (including not transforming) possible functions that can be applied to the two copies of the audio sample, resulting in 4 possible augmentation cases; 0vs1, 1vs1, 1vs2 and 2vs2. As a first step, we examined all possible combinations in the 0vs1 and 1vs1 cases without applying the same transformation

Table 2: This table presents the results of the best performing models (as reported in Section 4.1) Top results are specified in bold face. The first column of the table indicates the datasets on which the SSL backbone was pretrained on. E, F, Pa, P16 and P22, indicate data from the Ephnogram, Fpcgdb, Pascal, PhysioNet16 and PhysioNet22 datasets respectively. The SSL and fully-supervised baseline models are trained and evaluated on *In-Distribution* data from the respective dataset. The presented models are the best-performing models, based on results from the *In-Distribution* test data split. Once trained, they are then evaluated on out-of-distribution data originating from unseen datasets. The ‘All’ labels indicate that the PCG signals are classified based on the dataset’s original labels (P16 has only binary labels), whereas ‘Binary’ indicates that the signals are classified between normal and abnormal. The SSL-NoDs model refers to the backbone network which has not ‘seen’ data from the downstream task dataset during pretraining.

SSL Datasets	Model	In-Distribution				Out-of-Distribution		Out-of-Distribution	
		All		Binary		Binary		Binary	
		Acc	F1	Acc	F1	Acc	F1	Acc	F1
		<i>Pascal</i>				<i>PhysioNet2016</i>		<i>PhysioNet2022</i>	
—	Baseline	79.37	<u>48.37</u>	67.77	40.00	51.95	62.74	51.33	59.41
E, F, Pa, P16	SSL	76.87	42.18	31.25	47.61	63.55	74.88	53.24	64.44
E, F, Pa, P22	SSL	76.87	42.18	32.10	<u>42.25</u>	61.56	72.69	61.11	<u>73.64</u>
E, F, P16, P22	SSL-NoDs	75.62	39.06	31.25	40.00	59.88	<u>74.97</u>	58.33	72.06
all	SSL	81.25	53.12	35.93	47.61	67.13	79.09	62.11	74.72
		<i>PhysioNet2016</i>				<i>Pascal</i>		<i>PhysioNet2022</i>	
—	Baseline	—	—	88.64	93.09	55.00	40.00	49.85	60.59
E, F, Pa, P16	SSL	—	—	80.07	87.38	48.58	42.90	57.74	70.97
E, F, Pa, P22	SSL-NoDs	—	—	74.97	85.69	52.55	42.61	58.99	71.59
E, F, P16, P22	SSL	—	—	84.19	89.65	31.25	<u>47.62</u>	62.07	<u>78.07</u>
all	SSL	—	—	85.02	<u>90.31</u>	42.19	50.66	70.45	81.63
		<i>PhysioNet2022</i>				<i>Pascal</i>		<i>PhysioNet2016</i>	
—	Baseline	90.80	86.21	86.90	91.90	53.12	<u>53.12</u>	67.91	80.64
E, F, Pa, P16	SSL-NoDs	87.94	81.91	82.49	89.71	48.29	47.09	70.45	81.63
E, F, Pa, P22	SSL	88.55	82.83	82.83	89.96	51.42	48.64	71.07	<u>82.94</u>
E, F, P16, P22	SSL	85.37	78.06	78.06	87.67	31.25	47.61	74.97	85.70
all	SSL	89.31	<u>83.96</u>	83.67	<u>90.00</u>	48.44	54.79	74.97	85.70

twice. After evaluating the above we selected a subset of the augmentations leading to the top performing models and continued experimenting with 1vs2 and 2vs2 augmentation schemes. The models with the best results are the ones presented in Table 2 which are discussed in the next section.

However, the main aim of this study is to provide an evaluation of the most appropriate augmentations for PCG signal analysis. Due to the fact that by only presenting the combination of the augmentations leading to the best classification results could be misleading (since only the specific combination could pertain to said results), we present a plot depicting the frequency of augmentation occurrence in the top 75 experiments across all 3 downstream tasks and for both In-Distribution and OOD data. Specifically, we select the top 25 results for each task and present the occurrences for all 75 total experiments in Fig. 3. The evaluation results are quite interesting as several conclusions can be made. First of all, the application of low-pass filters seem to be dominant in both In-Distribution and OOD top experiments. This is a clear indicator that such filters should be applied towards increasing the robustness of a classifier. What is more, the application of uniform noise, random flip and scaling on the signal, also boosts the effectiveness of classifiers in all cases. Furthermore, we found that the best performing models in each of the 3 downstream tasks, had adopted the following augmentations during their pretraining:

- Pascal: high pass filter (pass band 250Hz, stop band 300 Hz) and random flip (p=0.7) vs inversion and uniform noise (mean 0, std 0.1),
- PhysioNet2016: high pass filter (pass band 250Hz, stop band 300 Hz) vs reverse
- PhysioNet2022: high pass filter (pass band 250Hz, stop band 300 Hz) vs random flip (p=0.7) and random scaling with a between 1.0 and 1.5

While the above augmentations agree, for the most part, with the distributions and number of occurrences in Fig. 3, they also support the findings in several previous contrastive SSL works [63, 72], in which stronger augmentations lead to improved results.

To further validate our results and to draw concrete conclusions regarding the importance of each applied transformation, we calculate Cohen’s d [73] for each implemented function. Cohen’s d provides a standardized measure of the effect size of each augmentation and allows the comparison of their

magnitude. Given two groups x_1 and x_2 , Cohen’s d is the difference in their means divided by the pooled standard deviation (s). Specifically, Cohen’s d is defined as:

$$d = \frac{\bar{x}_1 - \bar{x}_2}{s} \quad (3)$$

where the pooled standard deviation is defined as:

$$s = \sqrt{\frac{(n_1 - 1)s^2_1 + (n_2 - 1)s^2_2}{n_1 + n_2 - 2}} \quad (4)$$

and n_1, n_2 are the variances for each group respectively. The consensus on the interpretation of Cohen’s d is generally that its sign means to either a negative or positive effect, while a magnitude of $d = 0.01$ up to $d = 2.0$ corresponds to a very small or very large effect, respectively. To calculate Cohen’s d , we create two subgroups for each augmentation. Specifically, let a be an augmentation under consideration. The first group (x_1) contains all experiments where a was implemented, while the second group (x_2) consists of all experiments with the same set of augmentations but without a . For example, say that the augmentation under consideration is *Noise*. One experiment to include in the first group would be the *Noise vs Inversion* experiment. Therefore the corresponding experiment which should be added to the second group would be *None vs Inversion*. The same process can be repeated for all augmentations and for all runs, including *2vs2* experiments, as specified in Sec. 3.3. Accordingly, we calculate the effect of each augmentation based on the Out-of-Distribution Micro F1 scores for the PhysioNet2016 dataset, when trained on signals from PhysioNet2022. The magnitude of effect regarding each augmentation is presented in Table 1.

Interestingly enough, the statistics presented in Fig. 3, seem to agree with the effect sizes of each augmentation (Table 1). Based on Cohen’s d measure, the low-pass filters have the most important positive effect on robust SSL PCG learning. In simple terms, this means that the addition or application of low-pass cut-off filters during the pretraining phase of the encoder plays a significant role ($d > 1.0$) in learning robust representations. Additionally, the application of *Reverse* and *Inversion* (i.e Random Flip) has an overall positive effect on training, as shown by the positive d measure. What’s more, the balanced reversion of inversion of the signals (i.e Random Flip with a .5% chance), has the largest positive effect ($d \approx 1.8$), whereas the application of

only one of the above flip augmentations seems to have approximately no effect on training. Similarly, but to a less degree, scaling the signals by a small factor, assists the model in extracting meaningful representations. On the other hand, the addition of noise, the application of high-pass filters and large scaling, generally appear to have a negative effect. The intuition behind the negative effect of noise, is that since the selected signals derive from an already “noisy” dataset, the additive noise renders them meaningless.

In the next section we present numerical results for all downstream tasks and experiments.

4.2. Results

Table 2 presents the Accuracy and F1-Scores of the best performing models trained via contrastive SSL for all downstream tasks, including evaluation on OOD distribution data, as presented in Section 3.4. We perform a total of 4 cycles of SSL experiments, evaluating all augmentation combinations in each cycle. In each experiment cycle, we either use all available datasets or leave one labeled dataset out at a time. The first column of Table 2 denotes the datasets used during SSL training. In the same table, the ‘*Baseline*’ model refers to the fully-supervised model trained solely on data from the downstream ‘In-Distribution’ dataset. Due to the variance in the OOD results for the baseline model, we present the average of 5 total runs. Finally, the ‘SSL-NoDs’ model refers to the model which has not been pretrained with data originating from the dataset of the downstream task. All results are rated based on the F1-Scores on the ‘In-Distribution’ test splits and the adopted augmentations for each case are the ones mentioned in Section 4.1. The same models are then evaluated on the test splits of the OOD datasets.

4.3. Discussion

At a first glance, the benefits of SSL pretraining admittedly do not seem very compelling. When evaluating the model on the test data of the In-Distribution data, the baseline fully-supervised model outperforms the SSL models in 2 out of 3 cases. When trained on the PhysioNet2016 and PhysioNet2022 datasets the baseline surpasses the best SSL model by 2.78% and 1.9% respectively. However, the same does not hold in the case of the Pascal dataset, where the SSL model is able to outperform the baseline by 4.75% when evaluated on ‘All’ labels and by 7.61% in the ‘Binary’ task. Since the Pascal dataset is considerably smaller than the other 2, and arguably the hardest among the datasets, the above results validate the effectiveness of

pretraining a model on a large corpus of data, when available labeled data is not sufficient.

By diving further into the results, the true benefits of the proposed method begin to show. First of all, the drop in effectiveness between in-distribution and OOD data is apparent. Additionally, in all cases the baseline models appear to have overfit their training data distribution and fail to maintain their classification ability across distinct datasets. On the other hand, the models which have been pretrained via SSL yield far superior results. In all cases, the models trained with the proposed framework surpass the baseline by 11.68% on average and even outperform it by 21.04% in the case of the PhysioNet22 OOD task. Even more so, the SSL models were surprisingly able to surpass both the effectiveness of the baseline and their ‘In-Distribution’ counterpart, in the case of the Pascal OOD evaluation. Specifically, the downstream models trained on data from PhysioNet2016 and PhysioNet2022 were able to yield better results than the fully-supervised model trained solely on Pascal data. Furthermore, even though there is a decrease in effectiveness when the OOD datasets are left out during model pretraining, the SSL models continue to outshine the baseline across the board, with the exception of the case where the downstream task is the PhysioNet2022 data and models are evaluated on OOD data from Pascal. Finally, we would like to note that the above findings are aligned with the results of our preliminary SSL method [24] submitted in the PhysioNet2022 challenge, where the proposed model was able to avoid overfitting on the available training distribution and demonstrated adequate generalization effectiveness on completely hidden data.

5. Conclusions

This research presents a comprehensive and extensive evaluation of augmentation and transformations for pretraining neural networks, towards robust PCG classification. In addition to presenting the best performing combinations of augmentations, we also provide a summary of the most frequently appearing transformation functions in the top 75 overall experimental results. Our experiments suggest that the use of cutoff filters, particularly low pass filters, leads to the best performing models among several datasets, rendering them almost essential during such tasks. Furthermore, the addition of small random noise and inversion or reversal of the signal, also yields improved results. Finally, the numerical results of our experiments validate

our claims that contrastive SSL learning can induce robust and generalizable classifiers, as the drop in effectiveness when evaluating on previously unseen data is far less than that of a fully-supervised model. The proposed method however, does not come without drawbacks. Most importantly, to pretrain a model via SSL, most likely a large corpus of data must be available beforehand in order to enhance the representation extraction capabilities of the model. What's more, the implemented contrastive loss expects a large batch size to perform as expected, adding a computational constraint to the overall framework. In the future, we aim to enhance the adopted augmentation techniques, by adding novel functions or researching further parameters of the existing ones, expanding the downstream tasks by incorporating transfer learning problems, as well as applying it to other 1D biosignals such as EMG.

Acknowledgement

The work leading to these results has been funded by the European Union under Grant Agreement No. 101057821, project RELEVIVUM.

References

- [1] GBD 2017 Causes of Death Collaborators, Global, regional, and national age-sex-specific mortality for 282 causes of death in 195 countries and territories, 1980-2017: a systematic analysis for the Global Burden of Disease Study 2017, *Lancet* 392 (10159) (2018) 1736–1788. doi:10.1016/S0140-6736(18)32203-7.
- [2] F. A. Khan, A. Abid, M. S. Khan, Automatic heart sound classification from segmented/unsegmented phonocardiogram signals using time and frequency features, *Physiological Measurement* 41 (5) (2020) 055006. doi:10.1088/1361-6579/ab8770.
- [3] R. Jaros, J. Koutny, M. Ladrova, R. Martinek, Novel phonocardiography system for heartbeat detection from various locations, *Scientific Reports* 13 (1) (2023) 14392.
- [4] J. Fontecave-Jallon, K. Fojtik, B. Rivet, Is there an optimal localization of cardiomicrophone sensors for phonocardiogram analysis?, in: 2019 41st Annual International Conference of the IEEE Engineering in Medicine and Biology Society (EMBC), 2019, pp. 3249–3252. doi:10.1109/EMBC.2019.8857681.
- [5] N. Giordano, S. Rosati, M. Knaflitz, Automated assessment of the quality of phonocardiographic recordings through signal-to-noise ratio for home monitoring applications, *Sensors* 21 (21) (2021) 7246. doi:10.3390/s21217246.

- [6] C. M. Huisa, C. Elvis Supo, T. Edward Figueroa, J. Rendulich, E. Sulla-Espinoza, Pcg heart sounds quality classification using neural networks and smote tometk links for the think health project, in: A. Khanna, Z. Polkowski, O. Castillo (Eds.), Proceedings of Data Analytics and Management, Springer Nature Singapore, Singapore, 2023, pp. 803–811.
- [7] R. Kahankova, et al., A review of recent advances and future developments in fetal phonocardiography, *IEEE Reviews in Biomedical Engineering* 16 (2023) 653–671. doi:10.1109/RBME.2022.3179633.
- [8] B. Recht, R. Roelofs, L. Schmidt, V. Shankar, Do imagenet classifiers generalize to imagenet?, in: International Conference on Machine Learning, PMLR, 2019, pp. 5389–5400.
- [9] A. Ballas, C. Diou, Towards domain generalization for ecg and eeg classification: Algorithms and benchmarks, *IEEE Transactions on Emerging Topics in Computational Intelligence* 8 (1) (2024) 44–54. doi:10.1109/TETCI.2023.3306253.
- [10] C. J. Reed, S. Metzger, A. Srinivas, T. Darrell, K. Keutzer, Selfaugment: Automatic augmentation policies for self-supervised learning, in: Proceedings of the IEEE/CVF Conference on Computer Vision and Pattern Recognition (CVPR), 2021, pp. 2674–2683.
- [11] C. Liu, et al., An open access database for the evaluation of heart sound algorithms, *Physiological Measurement* 37 (12) (2016) 2181, publisher: IOP Publishing. doi:10.1088/0967-3334/37/12/2181.
- [12] M. A. Reyna, et al., Heart murmur detection from phonocardiogram recordings: The George B. Moody PhysioNet Challenge 2022, pages: 2022.08.11.22278688 (Apr. 2023). doi:10.1101/2022.08.11.22278688.
- [13] A. L. Goldberger, et al., PhysioBank, PhysioToolkit, and PhysioNet: components of a new research resource for complex physiologic signals, *Circulation* 101 (23) (2000) E215–220. doi:10.1161/01.cir.101.23.e215.
- [14] H. Lu, et al., A lightweight robust approach for automatic heart murmurs and clinical outcomes classification from phonocardiogram recordings, in: 2022 Computing in Cardiology (CinC), Vol. 498, IEEE, 2022, pp. 1–4.
- [15] J. Ding, J.-J. Li, M. Xu, Classification of murmurs in pcg using combined frequency domain and physician inspired features, in: 2022 Computing in Cardiology (CinC), Vol. 498, 2022, pp. 1–4. doi:10.22489/CinC.2022.065.
- [16] M. S. Knorr, J. P. Bremer, Using mel-spectrograms and 2d-cnns to detect murmurs in variable length phonocardiograms, in: 2022 Computing in Cardiology (CinC), Vol. 498, 2022, pp. 1–4. doi:10.22489/CinC.2022.224.

- [17] M. Araujo, et al., Maiby’s algorithm: A two-stage deep learning approach for murmur detection in mel spectrograms for automatic auscultation of congenital heart disease, in: 2022 Computing in Cardiology (CinC), Vol. 498, 2022, pp. 1–4. doi:10.22489/CinC.2022.249.
- [18] Y. Xu, X. Bao, H.-K. Lam, E. N. Kamavuako, Hierarchical multi-scale convolutional network for murmurs detection on pcg signals, in: 2022 Computing in Cardiology (CinC), Vol. 498, 2022, pp. 1–4. doi:10.22489/CinC.2022.439.
- [19] A. Elola, et al., Beyond heart murmur detection: Automatic murmur grading from phonocardiogram, IEEE Journal of Biomedical and Health Informatics 27 (8) (2023) 3856–3866. doi:10.1109/JBHI.2023.3275039.
- [20] K. He, X. Zhang, S. Ren, J. Sun, Deep residual learning for image recognition, in: Proceedings of the IEEE Conference on Computer Vision and Pattern Recognition (CVPR), 2016.
- [21] M. Alkhodari, S. Kamarul Azman, L. J. Hadjileontiadis, A. Khandoker, Ensemble Transformer-Based Neural Networks Detect Heart Murmur In Phonocardiogram Recordings, 2022. doi:10.22489/CinC.2022.035.
- [22] S. Choi, H.-C. Seo, C. Kyungmin, G.-W. Yoon, S. Joo, Murmur classification with u-net state prediction, in: 2022 Computing in Cardiology (CinC), Vol. 498, 2022, pp. 1–4. doi:10.22489/CinC.2022.072.
- [23] Z. Imran, E. Grooby, V. V. Malgi, C. Sitaula, S. Aryal, F. Marzbanrad, A fusion of handcrafted feature-based and deep learning classifiers for heart murmur detection, in: 2022 Computing in Cardiology (CinC), Vol. 498, 2022, pp. 1–4. doi:10.22489/CinC.2022.310.
- [24] A. Ballas, V. Papapanagiotou, A. Delopoulos, C. Diou, Listen2YourHeart: A Self-Supervised Approach for Detecting Murmur in Heart-Beat Sounds, in: 2022 Computing in Cardiology (CinC), Vol. 498, 2022, pp. 1–4. doi:10.22489/CinC.2022.298.
- [25] L. Ericsson, H. Gouk, C. C. Loy, T. M. Hospedales, Self-supervised representation learning: Introduction, advances, and challenges, IEEE Signal Processing Magazine 39 (3) (2022) 42–62. doi:10.1109/MSP.2021.3134634.
- [26] I. Misra, L. v. d. Maaten, Self-supervised learning of pretext-invariant representations, in: Proceedings of the IEEE/CVF conference on computer vision and pattern recognition, 2020, pp. 6707–6717.
- [27] A. v. d. Oord, Y. Li, O. Vinyals, Representation Learning with Contrastive Predictive Coding, arXiv:1807.03748 [cs, stat]ArXiv: 1807.03748 (Jan. 2019).
- [28] X. Liu, et al., Self-supervised learning: Generative or contrastive, IEEE Transactions on Knowledge and Data Engineering 35 (1) (2023) 857–876. doi:10.1109/TKDE.2021.3090866.

- [29] P. Kumar, P. Rawat, S. Chauhan, Contrastive self-supervised learning: review, progress, challenges and future research directions, *International Journal of Multimedia Information Retrieval* 11 (4) (2022) 461–488. doi:10.1007/s13735-022-00245-6.
- [30] Y. Zhang, B. Hooi, D. Hu, J. Liang, J. Feng, Unleashing the power of contrastive self-supervised visual models via contrast-regularized fine-tuning, in: M. Ranzato, A. Beygelzimer, Y. Dauphin, P. Liang, J. W. Vaughan (Eds.), *Advances in Neural Information Processing Systems*, Vol. 34, Curran Associates, Inc., 2021, pp. 29848–29860.
- [31] M. H. Rafiei, L. V. Gauthier, H. Adeli, D. Takabi, Self-supervised learning for electroencephalography, *IEEE Transactions on Neural Networks and Learning Systems* (2022) 1–15doi:10.1109/TNNLS.2022.3190448.
- [32] M. N. Mohsenvand, M. R. Izadi, P. Maes, Contrastive Representation Learning for Electroencephalogram Classification, in: *Proceedings of the Machine Learning for Health NeurIPS Workshop*, PMLR, 2020, pp. 238–253, iSSN: 2640-3498.
- [33] H. Banville, et al., Self-Supervised Representation Learning from Electroencephalography Signals, in: *2019 IEEE 29th International Workshop on Machine Learning for Signal Processing (MLSP)*, IEEE, Pittsburgh, PA, USA, 2019, pp. 1–6. doi:10.1109/MLSP.2019.8918693.
- [34] H. Banville, O. Chehab, A. Hyvärinen, D.-A. Engemann, A. Gramfort, Uncovering the structure of clinical eeg signals with self-supervised learning, *Journal of Neural Engineering* 18 (4) (2021) 046020.
- [35] D. Kostas, S. Aroca-Ouellette, F. Rudzicz, BENDR: Using Transformers and a Contrastive Self-Supervised Learning Task to Learn From Massive Amounts of EEG Data, *Frontiers in Human Neuroscience* 15 (2021).
- [36] A. Vaswani, N. Shazeer, N. Parmar, J. Uszkoreit, L. Jones, A. N. Gomez, L. Kaiser, I. Polosukhin, Attention is All you Need, in: I. Guyon, et al. (Eds.), *Advances in Neural Information Processing Systems*, Vol. 30, Curran Associates, Inc., 2017.
URL https://proceedings.neurips.cc/paper_files/paper/2017/file/3f5ee243547dee91fbd053c1c4a845aa-Paper.pdf
- [37] T. Mehari, N. Strodthoff, Self-supervised representation learning from 12-lead ECG data, *Computers in Biology and Medicine* 141 (2022) 105114. doi:10.1016/j.combiomed.2021.105114.
- [38] P. Sarkar, A. Etemad, Self-Supervised ECG Representation Learning for Emotion Recognition, *IEEE Transactions on Affective Computing* 13 (3) (2022) 1541–1554. doi:10.1109/TAFFC.2020.3014842.

- [39] J. Vazquez-Rodriguez, G. Lefebvre, J. Cumin, J. L. Crowley, Transformer-based self-supervised learning for emotion recognition, in: 2022 26th International Conference on Pattern Recognition (ICPR), IEEE, 2022, pp. 2605–2612.
- [40] D. Kiyasseh, T. Zhu, D. A. Clifton, CLOCS: Contrastive Learning of Cardiac Signals Across Space, Time, and Patients, in: Proceedings of the 38th International Conference on Machine Learning, PMLR, 2021, pp. 5606–5615, iSSN: 2640-3498.
- [41] J. Oh, H. Chung, J.-m. Kwon, D.-g. Hong, E. Choi, Lead-agnostic Self-supervised Learning for Local and Global Representations of Electrocardiogram, in: G. Flores, G. H. Chen, T. Pollard, J. C. Ho, T. Naumann (Eds.), Proceedings of the Conference on Health, Inference, and Learning, Vol. 174 of Proceedings of Machine Learning Research, PMLR, 2022, pp. 338–353.
- [42] H. Chen, G. Wang, G. Zhang, P. Zhang, H. Yang, CLECG: A Novel Contrastive Learning Framework for Electrocardiogram Arrhythmia Classification, IEEE Signal Processing Letters 28 (2021) 1993–1997. doi:10.1109/LSP.2021.3114119.
- [43] X. Lan, D. Ng, S. Hong, M. Feng, Intra-Inter Subject Self-Supervised Learning for Multivariate Cardiac Signals, Proceedings of the AAAI Conference on Artificial Intelligence 36 (4) (2022) 4532–4540, number: 4. doi:10.1609/aaai.v36i4.20376.
- [44] D. Xiong, D. Zhang, X. Zhao, Y. Zhao, Deep learning for emg-based human-machine interaction: A review, IEEE/CAA Journal of Automatica Sinica 8 (3) (2021) 512–533. doi:10.1109/JAS.2021.1003865.
- [45] Y. Liu, S. Zhang, M. Gowda, A Practical System for 3-D Hand Pose Tracking Using EMG Wearables With Applications to Prosthetics and User Interfaces, IEEE Internet of Things Journal 10 (4) (2023) 3407–3427. doi:10.1109/JIOT.2022.3223600.
- [46] Z. Lai, et al., Contrastive Domain Adaptation: A Self-Supervised Learning Framework for sEMG-Based Gesture Recognition, in: 2022 IEEE International Joint Conference on Biometrics (IJCB), 2022, pp. 1–7, iSSN: 2474-9699. doi:10.1109/IJCB54206.2022.10008005.
- [47] Y. Bengio, A. Courville, P. Vincent, Representation learning: A review and new perspectives, IEEE Transactions on Pattern Analysis and Machine Intelligence 35 (8) (2013) 1798–1828. doi:10.1109/TPAMI.2013.50.
- [48] M. Wang, W. Deng, Deep visual domain adaptation: A survey, Neurocomputing 312 (2018) 135–153.
- [49] F. Zhuang, et al., A comprehensive survey on transfer learning, Proceedings of the IEEE 109 (1) (2020) 43–76.
- [50] K. Zhou, Z. Liu, Y. Qiao, T. Xiang, C. C. Loy, Domain generalization: A survey, IEEE Transactions on Pattern Analysis and Machine Intelligence (2022).

- [51] A. Ballas, C. Diou, Multi-scale and multi-layer contrastive learning for domain generalization, *IEEE Transactions on Artificial Intelligence* (2024) 1–14 doi:10.1109/TAI.2024.3377173.
- [52] K. Weimann, T. O. F. Conrad, Transfer learning for ECG classification, *Scientific Reports* 11 (1) (2021) 5251, number: 1 Publisher: Nature Publishing Group. doi:10.1038/s41598-021-84374-8.
- [53] Z. He, et al., A novel unsupervised domain adaptation framework based on graph convolutional network and multi-level feature alignment for inter-subject ECG classification, *Expert Systems with Applications* 221 (2023) 119711. doi:https://doi.org/10.1016/j.eswa.2023.119711.
- [54] Z. Wan, R. Yang, M. Huang, N. Zeng, X. Liu, A review on transfer learning in EEG signal analysis, *Neurocomputing* 421 (2021) 1–14.
- [55] Q. She, et al., Improved domain adaptation network based on wasserstein distance for motor imagery eeg classification, *IEEE Transactions on Neural Systems and Rehabilitation Engineering* 31 (2023) 1137–1148. doi:10.1109/TNSRE.2023.3241846.
- [56] H. Zhao, Q. Zheng, K. Ma, H. Li, Y. Zheng, Deep representation-based domain adaptation for nonstationary eeg classification, *IEEE Transactions on Neural Networks and Learning Systems* 32 (2) (2021) 535–545. doi:10.1109/TNLS.2020.3010780.
- [57] P. Peng, et al., Domain adaptation for epileptic EEG classification using adversarial learning and Riemannian manifold, *Biomedical Signal Processing and Control* 75 (2022) 103555. doi:10.1016/j.bspc.2022.103555.
- [58] Z. Lan, O. Sourina, L. Wang, R. Scherer, G. R. Müller-Putz, Domain adaptation techniques for EEG-based emotion recognition: a comparative study on two public datasets, *IEEE Transactions on Cognitive and Developmental Systems* 11 (1) (2018) 85–94, publisher: IEEE.
- [59] T. Dissanayake, et al., Domain generalization in biosignal classification, *IEEE Transactions on Biomedical Engineering* 68 (6) (2021) 1978–1989. doi:10.1109/TBME.2020.3045720.
- [60] H. Hasani, A. Bitarafan, M. S. Baghshah, Classification of 12-lead eeg signals with adversarial multi-source domain generalization, in: *2020 Computing in Cardiology*, 2020, pp. 1–4. doi:10.22489/CinC.2020.445.
- [61] B.-Q. Ma, H. Li, W.-L. Zheng, B.-L. Lu, Reducing the Subject Variability of EEG Signals with Adversarial Domain Generalization, in: T. Gedeon, K. W. Wong, M. Lee (Eds.), *Neural Information Processing, Lecture Notes in Computer Science*, Springer International Publishing, Cham, 2019, pp. 30–42. doi:10.1007/978-3-030-36708-4_3.

- [62] A. Ballas, C. Diou, A domain generalization approach for out-of-distribution 12-lead ecg classification with convolutional neural networks, in: 2022 IEEE Eighth International Conference on Big Data Computing Service and Applications (BigDataService), 2022, pp. 9–13. doi:10.1109/BigDataService55688.2022.00009.
- [63] T. Chen, S. Kornblith, M. Norouzi, G. Hinton, A Simple Framework for Contrastive Learning of Visual Representations, in: Proceedings of the 37th International Conference on Machine Learning, PMLR, 2020, pp. 1597–1607, iSSN: 2640-3498.
- [64] A. Kazemnejad, P. Gordany, R. Sameni, Ephnogram: A simultaneous electrocardiogram and phonocardiogram database, PhysioNet (2021).
- [65] M. Cesarelli, M. Ruffo, M. Romano, P. Bifulco, Simulation of foetal phonocardiographic recordings for testing of FHR extraction algorithms, Computer Methods and Programs in Biomedicine 107 (3) (2012) 513–523. doi:10.1016/j.cmpb.2011.11.008.
- [66] P. Bentley, G. Nordehn, M. Coimbra, S. Mannor, The PASCAL Classifying Heart Sounds Challenge 2011 (CHSC2011) Results, <http://www.peterjbentley.com/heartchallenge/index.html>.
- [67] T. Chen, S. Kornblith, M. Norouzi, G. Hinton, A simple framework for contrastive learning of visual representations, in: International conference on machine learning, PMLR, 2020, pp. 1597–1607.
- [68] V. Papapanagiotou, C. Diou, A. Delopoulos, Chewing detection from an in-ear microphone using convolutional neural networks, Annual International Conference of the IEEE Engineering in Medicine and Biology Society. IEEE Engineering in Medicine and Biology Society. Annual International Conference 2017 (2017) 1258–1261. doi:10.1109/EMBC.2017.8037060.
- [69] B. Ginsburg, I. Gitman, Y. You, Large batch training of convolutional networks with layer-wise adaptive rate scaling (2018).
- [70] M. Abadi, et al., TensorFlow: Large-scale machine learning on heterogeneous systems, software available from tensorflow.org (2015).
URL <https://www.tensorflow.org/>
- [71] A. B. Yoo, M. A. Jette, M. Grondona, SLURM: Simple Linux Utility for Resource Management, in: D. Feitelson, L. Rudolph, U. Schwiegelshohn (Eds.), Job Scheduling Strategies for Parallel Processing, Lecture Notes in Computer Science, Springer, Berlin, Heidelberg, 2003, pp. 44–60. doi:10.1007/10968987_3.
- [72] B. Gopal, et al., 3KG: Contrastive Learning of 12-Lead Electrocardiograms using Physiologically-Inspired Augmentations, in: Proceedings of Machine Learning for Health, PMLR, 2021, pp. 156–167, iSSN: 2640-3498.
- [73] J. Cohen, Statistical power analysis for the behavioral sciences, Routledge, 2013.